Peptide Science

WILEY

PeptideScience

ARTICLE OPEN ACCESS

Disruption of the LRRK2-FADD Interface Using Constrained Peptides

Krista K. Alexander[1] | Michalis Kentros[2] | Leah G. Helton[1] | Dimitris Tantis-Tapeinos[2] | Timothy J. LeClair[1] | Fredejah T. Royer[1] | Neil J. Grimsey[1] | Alexia V. Polissidis[2] | Eileen J. Kennedy[1] | Hardy J. Rideout[2]

[1]Department of Pharmaceutical and Biomedical Sciences, College of Pharmacy, University of Georgia, Athens, Georgia, USA | [2]Laboratory of Neurodegenerative Diseases, Center for Clinical, Experimental Surgery and Translational Research, Biomedical Research Foundation of the Academy of Athens, Athens, Greece

Correspondence: Eileen J. Kennedy (ekennedy@uga.edu) | Hardy J. Rideout (hrideout08@gmail.com)

Received: 30 April 2024 | **Revised:** 29 June 2024 | **Accepted:** 1 July 2024

Funding: E.J.K. was supported by the Michael J. Fox Foundation for Parkinson's Research (8068.04 and 023920). Part of this work was supported by the Parkinson's and Movement Disorders Foundation (H.J.R. and A.V.P.).

Keywords: FADD | LRRK2 | Parkinson's disease | protein–protein interaction | stapled peptides

ABSTRACT

Mutations in the gene encoding leucine-rich repeat kinase 2 (*LRRK2*) are the most common cause of familial Parkinson's disease (PD). The reduced penetrance of mutations in the LRRK2 gene has also led to variants appearing in seemingly sporadic forms of the disease. Kinase inhibition effectively blocks neuronal death and small-molecule Class I inhibitors are proceeding through clinical trials in multiple PD cohorts. The toxic interaction between mutant LRRK2 and FADD lies downstream of its kinase activity and is required to induce neuronal death. The present study aimed to determine whether the FADD-LRRK2 interface could be disrupted and what effects this may have on neuroprotection. A series of constrained peptides were designed to mimic the alpha-helical protein interaction interface between the LRRK2 armadillo region and the death domain of FADD. These peptide-based protein–protein interaction inhibitors significantly reduced this interaction and blocked apoptotic death of primary neurons expressing G2019S-LRRK2. This work has identified novel constrained peptides that disrupt the LRRK2-FADD interface and downregulate mutant LRRK2-induced neuronal death in an allosteric manner, thereby providing a potential alternative therapeutic approach for PD.

1 | Introduction

Neuronal death induced by mutant forms of leucine-rich repeat kinase 2 (LRRK2), as demonstrated in viral in vivo or cellular overexpression models, is the result of a complex series of signaling events requiring intact kinase activity (e.g., [1]) as well as specific components of various cell death pathways [2]. We have previously shown that the baseline interaction between wild-type (WT) LRRK2 and the death adaptor protein FADD is strengthened by most pathogenic mutant forms of LRRK2; and this interaction serves to recruit and activate caspase-8 [3]. Further, it was shown that the increased interaction between mutant LRRK2 and FADD was downstream of LRRK2 kinase activity [3]. In addition, genetic ablation of kinase activity restored the interaction with FADD to WT LRRK2 levels. Subsequently, it was found that in addition to activating these components of the extrinsic death pathway, FADD/caspase-8 signaling in neurons activated downstream mitochondrial death cascades involving translocation of Bid and Bax to the mitochondria [2].

We have mapped the binding domain of LRRK2 that mediates the interaction with the FADD death domain to the armadillo

Krista K. Alexander, Michalis Kentros, and Leah G. Helton contributed equally to this work.

This is an open access article under the terms of the Creative Commons Attribution-NonCommercial-NoDerivs License, which permits use and distribution in any medium, provided the original work is properly cited, the use is non-commercial and no modifications or adaptations are made.

© 2024 The Author(s). *Peptide Science* published by Wiley Periodicals LLC.

region within the large N-terminal domain of LRRK2 [2]. Homology modeling of this region of LRRK2, coupled with molecular docking techniques, further refined the domain mapping to identify candidate residues that mediate this interaction. Targeting the LRRK2–FADD interaction using genetic or dominant negative approaches successfully reduced the protein–protein interface (PPI) and was neuroprotective in primary cultured cortical neurons [2, 3]. Further, deletion of the FADD-binding region within the ARM domain of LRRK2 reduced the recruitment of WT LRRK2 to overexpressed FADD death-effector filaments and prevented the induction of neuronal death by mutant LRRK2. Similarly, co-expression of mutant LRRK2 and a dominant negative fragment of the FADD death domain prevented the binding of LRRK2 with full-length FADD and was also neuroprotective [2].

In this work, we sought to explore whether the LRRK2-FADD PPI could be disrupted using constrained ("stapled") peptides. To accomplish this, a series of hydrocarbon-stapled peptides were designed based on a FADD-derived sequence that binds to LRRK2. We utilized the crystal structure of the FADD death domain and the model we previously constructed of the LRRK2-ARM region [2] to identify key residues that comprise the PPI. These hydrocarbon-constrained peptides were subsequently characterized for their ability to block the LRRK2-FADD interface.

Here, we show that a constrained peptide mimicking a portion of the modeled FADD-LRRK2 interface, termed FARM5, permeates cultured cells as well as primary cortical neurons. Further, it was found to disrupt the interaction between LRRK2 and FADD and results in neuroprotection in a cellular model of mutant LRRK2-PD. Critically, blocking the interaction between mutant LRRK2 and FADD in primary neurons by FARM5 prevents the initiation of a FADD-dependent cell death pathway and subsequent apoptotic neuronal death. Overall, these findings highlight a possible novel, non-catalytic strategy to inhibit LRRK2 from inducing neuronal apoptosis in Parkinson's disease (PD).

2 | Results

2.1 | Design and Synthesis of Constrained Peptides Targeting LRRK2 PPIs

Using the modeled binding interface between the LRRK2 ARM region and the death domain of FADD as a template, key residues were identified that comprised the binding interface with LRRK2 (Figure 1A,B). Multiple structural studies [4, 5] of LRRK2 using cryo-EM have been reported since we first characterized this PPI based on our homology modeling and molecular docking (see [2]). The homology model we built previously is a restricted fragment within the ARM repeat domain, based on domain and subdomain co-precipitation with FADD [2]. A so-called "hinge-helix" reported [5] slightly beyond our modeled region is conceivably predicted by a kink formed within the α-helix in this region [2] in our model. This FADD-derived helix (residues 173–190) was used for the library design of FADD Armadillo domain (FARM) peptides (Figure 1B). The FARM peptide library was synthesized using standard solid-phase peptide synthesis (SPPS). The staple was generated by incorporating (*S*)-2-(4-pentenyl)alanine at *i*, *i* + 4 positions and cyclized using ring-closing metathesis (RCM) chemistry while on solid support (Figure 1C). The library (FARM1-FARM5) was generated by integrating the staple at different positions along the predicted nonbinding face of the helix to stabilize side chain residues anticipated to interact with LRRK2 (Figure 1D). In addition, single Lys residues were added to the terminal ends of each peptide to increase the overall positive net charge to promote cell permeation.

2.2 | Constrained Peptides Disrupt the PPI Between LRRK2 and FADD

We have previously shown that the deletion of a region within the LRRK2 armadillo region disrupts the interaction with FADD and is neuroprotective [2]. Here, we took an alternative approach to disrupting this PPI by the competitive binding of a conformationally constrained peptide based on the LRRK2-binding region in the FADD death domain.

To determine whether the peptides could permeate cells, we quantified the uptake of FAM-labeled stapled peptides in HEK293T cells using flow cytometry. Each of the FARM peptides demonstrated a shift in increased fluorescence signal relative to the untreated cell control with FARM5 demonstrating the greatest fluorescence shift (Figure 2A). Confocal cell imaging was also performed using HEK293T cells treated with FAM-labeled FARM peptide (in this representative image, FARM5) or its native control (a peptide with the identical sequence, but without the staple) for 6 h prior to imaging. While the non-stapled control peptide was not found to permeate cells, a clear diffuse cytoplasmic fluorescent signal was observed throughout cells treated with FARM5 (Figure 2B). On the basis of these results, we selected FARM5 as the lead candidate peptide to proceed with further characterization.

Next, we measured whether the constrained peptides could bind LRRK2 in vitro. Biotinylated FARM5 peptide was incubated in streptavidin-coated ELISA plates at a concentration of 10 μM, after which protein extract (0.1, 1, or 10 μg total protein) from HEK293T cells overexpressing full-length G2019S-LRRK2 or G2019S-LRRK2 containing a deletion in the armadillo region corresponding to the predicted FADD-binding site in LRRK2 (see [2]). LRRK2 was detected using HRP-conjugated anti-LRRK2 (clone N241; with a C-terminal epitope). FARM5 successfully captured full-length LRRK2, but not LRRK2 harboring the FADD-binding motif deletion (Figure S2B).

Using this cell background and protein purification strategy, we then assessed whether this peptide library (FARM1-FARM5) could disrupt the interaction between overexpressed Flag G2019S-LRRK2 and V5-FADD by co-immunoprecipitation (Figure 3). Flag-LRRK2 was purified on anti-Flag resin and the eluate as well as the protein extract (input) was separated by SDS-PAGE, and the membranes were probed for V5 (FADD) and Flag (LRRK2). The transfected cells were treated with the indicated peptide (10 μM) for a total of 48 h prior to collection. At this time point, a reduction was found in the amount of FADD that co-purified with G2019S-LRRK2 for cells treated with FARM5 when normalized to the amount of immunoprecipitated Flag-LRRK2 (Figure 3A,B). The experiment was

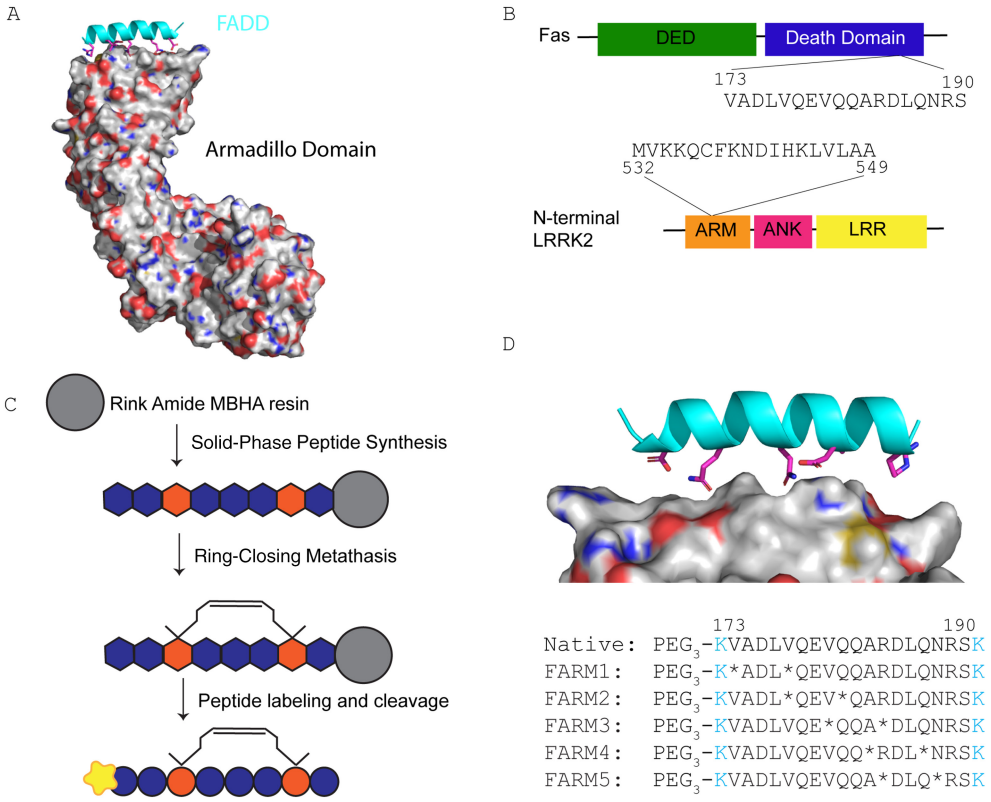

FIGURE 1 | Design and structure of constrained peptides targeting the LRRK2-FADD PPI. (A) Structural representation of the region of the LRRK2 ARM domain in which the FADD-binding motif is located, shown with the fragment of the FADD death domain that binds LRRK2. (B) Highlight schematic of the relevant binding domains within LRRK2 and FADD, and the corresponding amino acid sequence that mediates this PPI is highlighted. (C) Schematic representation of the solid-phase peptide synthesis, highlighting the placement of the synthetic amino acids for the placement of the peptide staple. (D) Sequences of the five stapled peptides synthesized for this study, with the position of the synthetic residues in each peptide indicated by an asterisk.

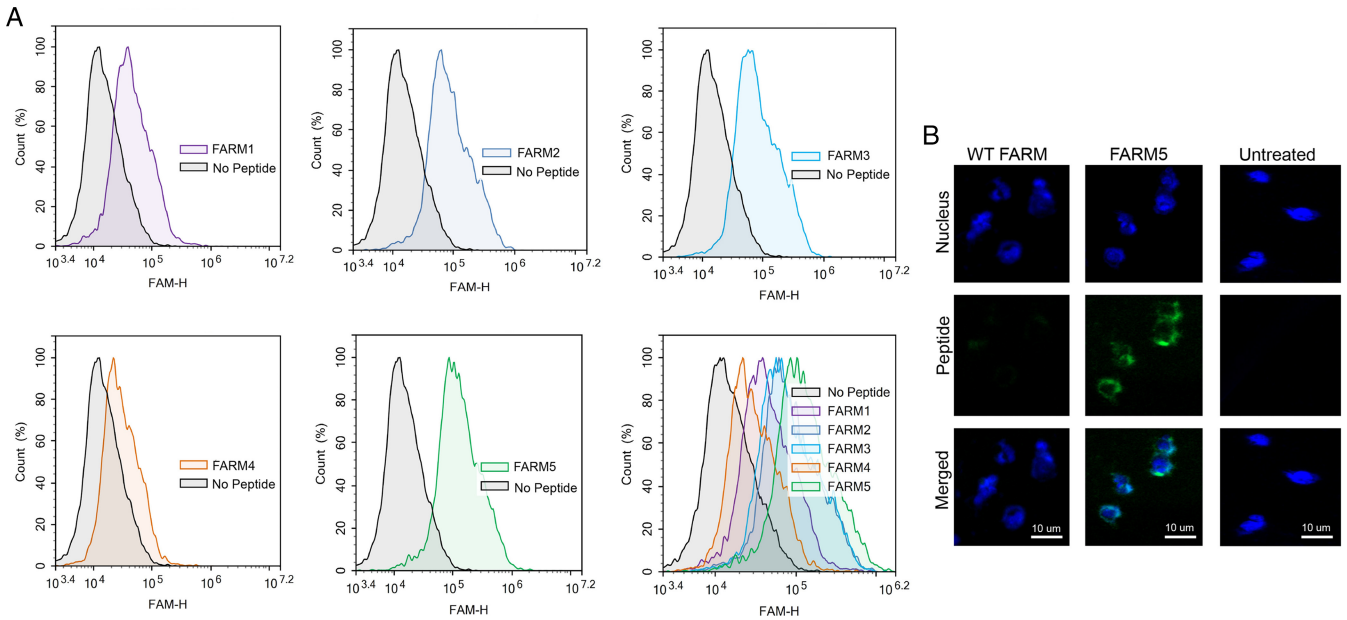

FIGURE 2 | Cellular uptake of stapled versus native peptides. (A) HEK293 cells were treated with 5 μM of each fluorescently labeled peptide for 4 h before analysis. Data were captured using 10,000 cells on an Agilent NovoSampler Q and analyzed using NovoExpress Software. Stapled peptide FARM5 showed the greatest increase in fluorescent shift compared to the other peptides. An overlay of each condition in (A) is shown in the panel on the lower right. These data highlight that the FARM5 peptide has the strongest cell uptake compared to the other peptides from the initial library. Graphs are representative of $n = 2$. (B) Representative confocal image of HEK293T cells treated for 4 h with 5 μM FARM5, showing a largely diffuse cytoplasmic distribution. In contrast, very little uptake is observed in cells treated with "WT-FARM5," which contains the same sequence, but no hydrocarbon staple. Scale bar = 10 μm.

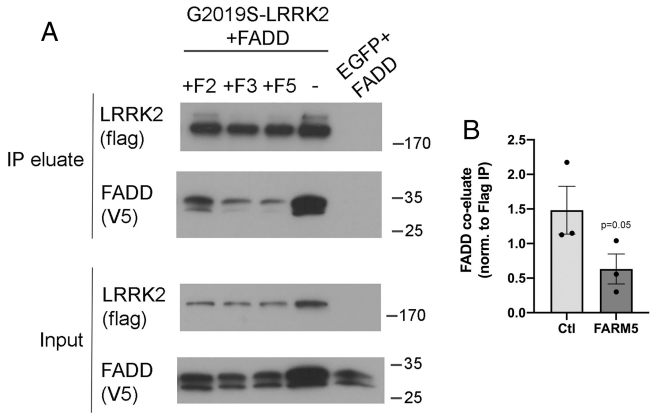

FIGURE 3 | Disruption of the LRRK2-FADD PPI by targeted stapled peptides. (A, B) HEK293T cells were transiently transfected with Flag G2019S-LRRK2 and V5-tagged FADD. Forty-eight hour after transfection the cells were treated with vehicle or the indicated peptide (10 μM) and incubated for a further 48 h. The cells were washed and processed for co-immunoprecipitation using Flag antibody-coated resin. The eluate was probed for precipitated LRRK2 (Flag) and co-eluting FADD (V5). Both FARM3 and FARM5 reduced the interaction between LRRK2 and FADD, when normalized to the amount of Flag-LRRK2 precipitated, and to a lesser extent FARM2, compared to control-treated cells. After observing enhanced cell uptake of FARM5 (see Figure 2), we proceeded with this peptide for further analyses. We performed an additional two independent experiments assessing the co-elution of FADD and LRRK2 with and without treatment with FARM5 (10 μM). The band intensities from the replicate blots of cells treated with FARM5 show the relative levels of FADD co-eluting with LRRK2; $p = 0.05$.

performed in triplicate and quantified after normalization to the amount of Flag-LRRK2 eluted, demonstrating that the difference in co-eluted FADD reached the threshold of statistical significance (Figure 3B, $p = 0.05$). We assessed the dose-dependency of the disruption of this interaction by FARM5 over a 24-h period and found a progressive reduction in the LRRK2-FADD PPI with increasing doses from 0.1 to 10 μM (Figure S3). Taken together, the fact that each of the tested peptides was able to disrupt the target PPI in cells, plus the apparent increased uptake, we made an arbitrary choice to proceed with FARM5 for subsequent experiments to examine the potential neuroprotective effects of LRRK2-FADD disruption. Other peptides in this library, which differed by the placement of the peptide staple, were also able to reduce the LRRK2-FADD interaction (Figure 3A); however, when taken together with the cellular update date, we elected to focus on the FARM5 peptide.

2.3 | Disruption of the LRRK2-FADD PPI Is Neuroprotective

We and others have previously shown that overexpression of mutant LRRK2 (G2019S or other pathogenic mutations) in primary cortical neurons results in apoptotic death of neurons [6]. We next sought to determine whether FARM5 could effectively block the apoptotic death of primary neurons induced by pathogenic LRRK2. In these experiments, mouse embryonic cortical neurons were transiently transfected with G2019S-LRRK2 and treated with a concentration gradient of the FARM5 peptide (0.5–10 μM), and the percentage of Flag (LRRK2)-positive neurons with apoptotic nuclei was determined. In cultures of neurons expressing G2019S-LRRK2, apoptotic Flag-positive neurons with characteristic fragmented and condensed nuclear apoptotic features were observed as has been reported previously [2]. In contrast, neurons expressing G2019S-LRRK2 treated with either 1 or 10 μM FARM5 showed reduced evidence of apoptotic neuronal death (Figure 4A), with the lowest concentration, 0.1 μM of FARM5, having no significant effect. This supports the notion that disrupting the LRRK2-FADD PPI with a FADD-derived constrained peptide may serve to protect primary neurons from the cell-autonomous death pathway triggered by the overexpression of mutant LRRK2.

3 | Discussion

In the present study, we extended our previous work characterizing the critical PPI between LRRK2 and the cell death adaptor protein FADD underlying the apoptotic death of neurons exogenously expressing pathogenic mutant forms of LRRK2. We show here that constrained peptides mimicking a helix derived from the FADD death domain that binds to the LRRK2 ARM domain can effectively disrupt this PPI, thereby inhibiting apoptotic death of primary neurons overexpressing the pathogenic mutant form of LRRK2 (G2019S). Given the evidence that LRRK2 may also play a vital role in the more common idiopathic forms of the disease (i.e., iPD) where WT LRRK2 is present [7], it will be critical to determine if this PPI-targeting approach can also demonstrate protection in cellular and in vivo models of iPD. At this point, it remains unknown whether the LRRK2-FADD PPI is also required for neuronal loss in iPD; and conversely, it is also not known what key phospho-substrate(s) of LRRK2 are required for the death of dopaminergic neurons. Moreover, since we address only the cell-autonomous neuronal death signaling triggered by mutant LRRK2, any potential therapeutic approach targeting this PPI may also need to consider alternative non-cell-autonomous mechanisms (e.g., contributions from peripheral and/or infiltrating immune cells) that contribute to the ultimate loss of dopaminergic neurons in PD since it is possible that additional LRRK2 protein interactors may be required.

It was recently demonstrated that Rab10 interacts with the ARM repeat region of LRRK2 [8], and thus the inhibitory strategy presented in this work may have implications on the docking of Rab10. The first binding motifs, binding preferentially non-phosphorylated Rab GTPases (Rab8a, Rab10, Rab29), are located within the 350–550 amino acid region of the LRRK2 ARM, adjacent to the region where we had previously mapped binding of FADD, between amino acids 500 and 550 [2]. As Rab29 in particular has been reported to enhance the activity of LRRK2 (see [8]), freeing up a potential binding region for Rab29 within the ARM region of LRRK2 (by displacing FADD binding in this region) may alter the downstream effect on LRRK2 activation. Future studies are needed to further explore the effects of other protein interactions on the ARM region of LRRK2.

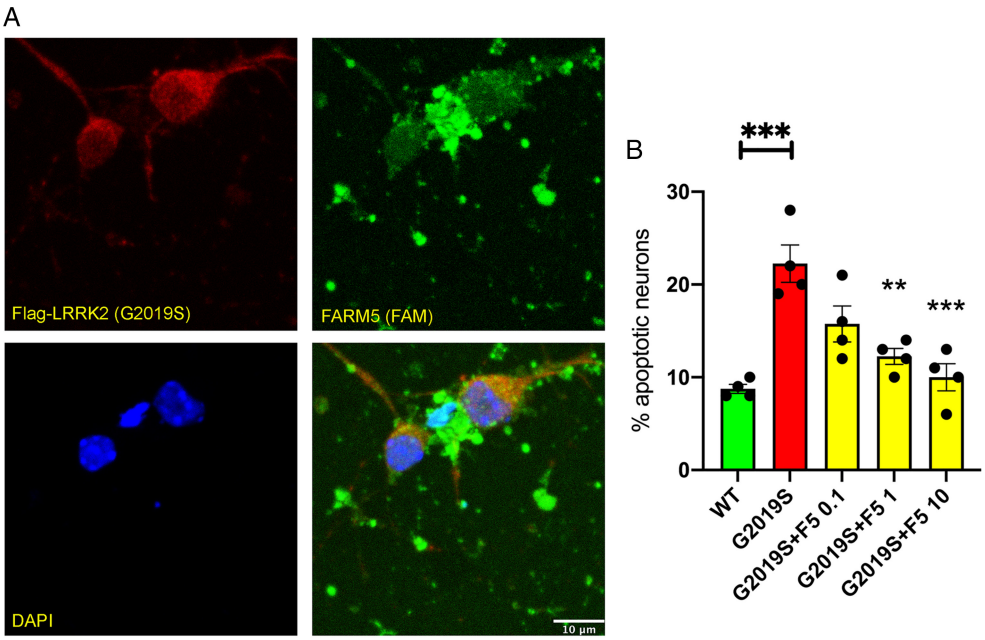

FIGURE 4 | Stapled peptides block apoptotic death of neurons expressing G2019S-LRRK2. (A) Primary embryonic cortical neurons were transiently transfected with Flag-LRRK2 (WT or G2019S) and subsequently treated with the indicated concentrations of FAM-tagged FARM5. The peptide was replenished after 24 h, and the total treatment period was 48 h. The neurons were fixed and processed for anti-Flag immunostaining with DAPI as a nuclear counterstain. Shown is a representative confocal micrograph of two neurons expressing G2019S-LRRK2 (Flag, red) and treated with 1 μM FARM5 (green channel). (B) The percentage of transfected neurons with apoptotic nuclear features was determined in a blinded fashion. The plots represent the mean apoptotic neurons (±SEM) from four technical replicates of one of three biological replicates (independent culture preps). $^{**}p < 0.01$; $^{***}p < 0.001$, ANOVA with Tukey's HSD post hoc test for pairwise comparisons.

Mutant LRRK2-induced PD likely involves multiple cell and non-cell-autonomous mechanisms in the pathogenesis of the disease, given its expression and known roles in both neuronal and non-neuronal cells [9]. The enriched primary neuronal model that we have employed, like other groups have also reported, elicits a cell-autonomous neuronal death, which is not to say that non-cell-autonomous mechanisms are not equally vital to the disease pathogenesis or progression. It is also critical to note that this acute model of neuronal death induced by mutant LRRK2 (G2019S or other pathogenic mutants) requires the overexpression of the transgene in primary neurons. Neuronal death is generally not observed at baseline, at endogenous expression levels of mutant LRRK2 in neurons (e.g., in iPS-derived dopamine neurons), at least during the acute time periods employed in the literature. Therefore, in these models an additional exogenous stressor would likely be needed as well. We have previously shown that the disruption of this PPI is effective not only against neuronal death elicited by G2019S-LRRK2 expression, but also other pathogenic LRRK2 variants [2, 10]. The highest concentration of FARM5 restored neuronal death to baseline levels (see Figure 4) within the isolated, cell-autonomous, cellular model. It will be critical to also determine if this PPI regulates or underlies LRRK2-dependent degeneration mediated by signaling in other non-neuronal cell types.

Several advantages of using constrained peptides include their ability to bind large protein surfaces such as those in PPIs due to the large surface area presented by the peptide, but also their high affinity, specificity, and low immunogenicity [11]. While these peptides were shown to permeate cells and neurons, a major hurdle still exists in delivering peptides across the blood–brain barrier (BBB); however, utilization of alternative delivery methods may overcome some of these challenges. Nonetheless, LRRK2 also plays an important role in peripheral tissues and immune cells in PD [12]. Stapled peptides targeting LRRK2 dimers have been recently described, reducing dimer formation, kinase activity, and neuronal death [13]. LRRK2 kinase inhibitors have already entered clinical trials for both LRRK2-PD as well as idiopathic PD [14]; and early trials have begun assessing the potential of LRRK2 antisense oligonucleotides as well. Considering that direct pharmacological inhibition of LRRK2 activity with ATP-competitive compounds can lead to pathological changes in the lung [15] and a redistribution to microtubule-bound skein-like filaments [4, 16], the development of alternative strategies to inhibit LRRK2 signaling may serve as complementary therapeutic approaches to disrupt LRRK2-induced neuronal loss.

4 | Materials and Methods

4.1 | Peptide Synthesis

All synthesis solvents and reagents used were high-performance liquid chromatography (HPLC) grade and purchased from Fisher, Sigma-Aldrich, Novabiochem, or ChemPep. The peptides were synthesized using standard Fmoc SPPS. Synthesis was performed on a rink amide MBHA resin using standard Nα-Fmoc amino acids. To synthesize the peptides, the MBHA resin was first calibrated by agitation in 1 mL of *N*- methylpyrrolidinone (NMP) for 10 min. Peptides were then

deprotected for 25 min with agitation. The deprotecting solution used contained 25% (v/v) piperidine and 75% (v/v) NMP. After each deprotection, the resin was washed three times for 30 s in NMP with agitation prior to coupling. Coupling was performed using 10 equivalents of each Nα-Fmoc amino acid, 9.9 equivalents of 2-(6-chloro-1*H*-benzotriazole-1-yl)-1,1,3,3-tetra methylammonium hexafluorophosphate (HCTU in NMP), and 20 equivalents of *N*,*N*-diisopropyl ethylamine (DIEA) as the catalyst for the reaction. Each amino acid coupling reaction was performed for 45 min with agitation. To couple the olefinic amino acid, 4 equivalents of (*S*)-*N*-Fmoc-2-(4-pentenyl) alanine (S_5) were incorporated into the sequence using 3.9 equivalents HCTU and 20 equivalents DIEA. Olefinic amino acid coupling was performed for 45 min with agitation. Following S_5 addition, each sequence was cyclized by RCM. To perform the RCM, 1,2-dichloroethane (DCE) and 0.4 equivalents of first-generation Grubbs were added to the resin with agitation for two separate 1-h cycles. After cyclization, 4 equivalents of Fmoc-11-amino-3,6,9-trioxaundecanoic acid (PEG_3) were added to the resin with 3.9 equivalents of HCTU, and 20 equivalents of DIEA. To label each peptide, 2 equivalents of 5,6-carboxyfluorescein (FAM) in dimethylformamide (DMF), 1.8 equivalents of HCTU, followed by 4.6 equivalents of DIEA were added to each resin with overnight agitation. Following overnight labeling, peptides were cleaved from the resin using 95% (v/v) trifluoracetic acid (TFA), 2.5% (v/v) triisopropylsilane (TIS), and 2.5% (v/v) distilled water. To cleave the peptides from the resin, the solution was rotated for 5 h at room temperature and precipitated via centrifugation at 4°C in methyl-tert-butyl ether. The supernatant was removed from each peptide, and pellets were allowed to dry using continuous airflow overnight while protected from light.

4.2 | Peptide Characterization

Following overnight drying, peptide pellets were diluted in 1 mL methanol and filtered using a 45-μm syringe filter. Peptides were then separated using an Agilent 1200 reverse-phase HPLC (RP-HPLC) on a Zorbax analytical SB-C18 column. For this RP-HPLC, the mobile phase linear gradient used was 10%–100% water to acetonitrile and 0.1% TFA. The flow rate used was 0.5 mL/min. To characterize the peptides, an Agilent 6120 Single Quadrupole electrospray ionization mass spectrometer (ESI-MS) was used. Purification of each peptide was carried out over a semi-preparatory column with a flow rate of 4 mL/min and with the same mobile phase as previously described [4]. To confirm peptide purity, final ESI-MS assays were performed (Figures S1–S3). Peptide molecular weights were used to characterize each product. The N-terminal intrinsic qualities were used to quantify the concentration of each peptide at 495 nm. The sequences and molecular weights of each peptide are shown in Table 1.

4.3 | Flow Cytometry

HEK293 cells (CRL1573, ATCC) were cultured and grown in complete (10% fetal bovine serum [FBS], 1.1% penicillin–streptomycin–glutamine) phenol-red-free RPMI 1640 media (Gibco) at 500,000 cells per well in 6-well plates (Falcon). After achieving full confluency, cells were treated with 5 μM of each fluorescently labeled peptide (FARM1, FARM2, FARM3, FARM4, FARM5) for 4 h before analysis. Untreated HEK293 cells were used as the control for data analysis. Following each treatment, cells were removed from the plates using trypsin and neutralized using fresh media. Cells were then centrifuged and resuspended in fresh, complete phenol-red-free RPMI 1640 media containing 25 mM HEPES (pH 7.4) in 1.5-mL Eppendorf tubes (VWR) for flow cytometry analysis. An Agilent NovoSampler Q flow cytometer was used to conduct the experiment, and the data were analyzed using the NovoExpress Software. During each experiment, 10,000 cells were counted and a gate for non-aggregating cells was defined. Wavelengths 488 nm (excitation) and 525 nm (emission) for the FITC channel were used. For each peptide, the experiment was conducted in duplicate.

In parallel, cellular uptake of the stapled peptides was demonstrated by fluorescence imaging. HEK293 cells (CRL-1573) were cultured and grown in Dulbecco's modified Eagle's medium (DMEM) (Corning) supplemented with 10% FBS (HyClone) and 1% penicillin–streptomycin (Gibco). To perform uptake experiments, 8-well chamber slides (Nunc Lab-Tek) were treated with poly-L-lysine solution (Sigma-Aldrich) at a 1:10 dilution with sterile water for 5 min. The solution was then aspirated, and the chambers were washed once with sterile water and further aspirated. The chamber slides were then placed in a 37°C incubator for 2 h. After 2 h, 20,000 HEK293 cells were added to each chamber and allowed to grow overnight. The next day, 5 μM FAM-labeled FARM WT and FARM5 treatments were added to the HEK293 cells for 4 h. After 4 h, cells were washed once in PBS. Cells were then permeabilized and fixed using 4% paraformaldehyde and 0.1% Triton solution for 10 min. This solution was then aspirated, followed by nuclear staining with 0.1 μg/mL Hoechst 34580 for 5 min. Cells were then washed and aspirated,

TABLE 1 | The sequence and molecular weight of each peptide.

FAM-labeled peptide	Sequence	Molecular mass (predicted)	Molecular weight (observed)
FARM1	5(6)FAM-PEG_3-K*ADL*QEVQQARDLQNRSK	2924.2	2924.4
FARM2	5(6)FAM-PEG_3-KVADL*QEV*QARDLQNRSK	2895.2	2895.0
FARM3	5(6)FAM-PEG_3-KVADLVQE*QQA*DLQNRSK	2867.1	2866.8
FARM4	5(6)FAM-PEG_3-KVADLVQEVQQ*RDL*NRSK	2923.2	2922.6
FAMR5	5(6)FAM-PEG_3-KVADLVQEVQQA*DLQ*RSK	2852.2	2851.8

Note: Red asterisks (*) symbolize S_5 residues.

followed by mounting with PermaFluor (PerkinElmer), covered with a coverslip, and imaged using a Zeiss Confocal Microscope at 10×.

4.4 | In Vitro Binding

To demonstrate the binding of FARM5 to LRRK2 in vitro, HEK293T cells (obtained from the laboratory of Prof. L. Stefanis; BRFAA, Athens, Greece) were transiently transfected (as before) with full-length Flag-tagged G2019S-LRRK2 or G2019S-LRRK2 with a deletion of the predicted FADD-binding motif (GS-del) as described previously [2]. Following 48 h after transfection, cell extracts were prepared using lysis buffer (see above). Twenty-four hours earlier, 96-well ELISA microplates were coated overnight at room temperature with streptavidin (SA) as described [17]. The next day, the wells were washed with 1× ELISA wash buffer and incubated with 10 μM biotinylated FARM5 for 1 h at 37°C followed by another three washes with 1× ELISA wash buffer. Next, increasing amounts of protein extract from cells expressing G2019S-LRRK2 or its corresponding deletion mutant (GS-del) were incubated in the FARM5-coated wells for 2 h at 37°C, followed by further washing. For both protein extracts, 0.1, 1, or 10 μg of total protein was added to the wells pre-coated with FARM5. After incubation with the protein extracts, the wells were washed and incubated with anti-LRRK2 detection antibodies (clone N241), preconjugated in house with HRP, for 1 h at room temperature. Following three washes with ELISA wash buffer, the wells were incubated at room temperature for 5 min with ECL-femto chemiluminescent substrate (Pierce Supersignal Femto). The signals were acquired using a Tecan Spark 10 M microplate reader.

4.5 | Plasmids and Cell Culture

Plasmids used for the assessment of the LRRK2-FADD PPI, as well as the overexpression of mutant LRRK2 in primary cortical neurons, were as described [2]. Human LRRK2 cDNA (from [3]) was PCR-amplified and subcloned into pcDNA3.1(+) with an N-terminal Flag epitope tag. The G2019S and R1441C pathogenic mutations were introduced using site-directed mutagenesis (QuikChange; Agilent Technologies) as per the manufacturer's instructions, and fully sequenced to ensure no errors were introduced. N-terminal V5-tagged FADD expression constructs were used as previously described [2, 10].

HEK293T cells were cultured as described [2] in DMEM growth medium (high glucose) plus 10% FBS and antibiotics. For the transient transfection of LRRK2 and FADD cDNA, we employed the Ca_2PO_4 DNA precipitation method. Embryonic day 16 (E16) pregnant C57BL mice were used in this study, with primary cortical neurons prepared as described [2]. Briefly, cortices were removed and cut into small pieces followed by enzymatic digestion (trypsin 0.05% and 100 μg/mL DNAse) and mechanical dissociation. Cells were centrifuged and counted and plated on poly-D-lysine–coated glass coverslips at a density of 150,000/cm^2 in BrainPhys neuronal culture medium (StemCell Technologies) supplemented with SM1 Neuronal Supplement (StemCell Technologies), L-glutamine (0.5 mM), and penicillin/streptavidin. After 3–4 DIV, neurons were transfected using Lipofectamine 2000 (ThermoScientific) as per the manufacturer's instructions. Neurons were transiently transfected with Flag-tagged WT or mutant (G2019S) human LRRK2 (as described previously [2]).

4.6 | Assessment of LRRK2-FADD Interaction

We undertook co-immunoprecipitation to determine the effects of the stapled peptides on the LRRK2-FADD PPI as previously described [2]. Briefly, 10-cm plates of HEK293T cells transiently expressing Flag-WT or mutant LRRK2 and V5-FADD (at a 3:1 ratio), and treated with different concentrations of FARM peptides (as indicated in the figure legends), were washed in PBS and lysed in co-IP buffer (20 mM HEPES, pH 7.4; 150 mM NaCl; 0.1% NP40; 2 mM EGTA; 2 mM $MgCl_2$; 10% glycerol, pH 7.2; protease and phosphatase cocktail [Agilent Technologies]) for 30 min on ice followed by 15 strokes with a Dounce glass homogenizer, and centrifugation at 13,000 rpm for 15 min to remove cellular debris. Following preclearing with IgG-coupled beads, 40 μL of washed anti-Flag resin (Sigma-Aldrich) per mg of protein was added, and the samples incubated under rotation overnight at 4°C. The following morning, the beads were centrifuged and washed a total of 5× with co-IP buffer, before elution in 2× SDS sample buffer at 95°C for 10 min. The eluate (and input) was separated by SDS-PAGE and membranes were probed with anti-Flag (LRRK2) and V5 (FADD).

4.7 | Assessment of Neuronal Death

The following day after transfection, we initiated the treatment of neurons with FAM-tagged stapled peptides (at 0.1–10 μM final concentration). We replenished the peptides in the neuronal medium after 24 h at the indicated concentrations. After 3 days of transfection and 2 days of treatment, the coverslips were washed in PBS and fixed in 3.7% paraformaldehyde for 20 min at 4°C. The neurons were processed for immunofluorescence labeling with the following antibodies: GFP (chicken; Abcam), Flag (M2 mouse; Sigma-Aldrich), and DAPI nuclear stain. Mounted coverslips were imaged on a Leica TSP5 multiphoton confocal microscope, and the Z-stacks were processed in FIJI/ImageJ and Adobe Photoshop. For the quantification of apoptotic neuronal profiles, we used the approach described by Antoniou et al. [2]. Briefly, individual Flag-positive neurons were assessed by a researcher blinded to the experimental conditions. The corresponding DAPI signal was evaluated in each Flag-positive neuron; and cells exhibiting condensed chromatin, fragmented into two or more "apoptotic bodies" were considered to be nonviable (i.e., apoptotic).

4.8 | Antibodies

We used the following antibodies in the current study: Flag (mouse clone M2; Sigma-Aldrich #F3165), V5 (rabbit; Sigma-Aldrich #V8137), GFP (chicken; Abcam #ab13970), phosphorylated (T73) Rab10 (rabbit clone MJF-R21; Abcam #ab230261), total Rab10 (rabbit; Abcam #ab237703), LRRK2 (mouse clone

N241; NeuroMab #75–253), LRRK2 (rabbit clone UDD3; Abcam), pS1292-LRRK2 (rabbit clone MJFR 19-7-8; Abcam #ab203181).

Acknowledgments

E.J.K. is supported by the Michael J. Fox Foundation for Parkinson's Research (8068.04 and 023920). Part of this work was supported by the Parkinson's and Movement Disorders Foundation (H.J.R. and A.V.P.).

Conflicts of Interest

The authors declare no conflicts of interest.

Data Availability Statement

All data generated in this study will be made reasonably available according to requests made to the corresponding authors.

References

1. E. Greggio, S. Jain, A. Kingsbury, et al., "Kinase Activity Is Required for the Toxic Effects of Mutant LRRK2/Dardarin," *Neurobiology of Disease* 23, no. 2 (2006): 329–341.

2. N. Antoniou, D. Vlachakis, A. Memou, et al., "A Motif Within the Armadillo Repeat of Parkinson's-Linked LRRK2 Interacts With FADD to Hijack the Extrinsic Death Pathway," *Scientific Reports* 8, no. 1 (2018): 3455.

3. C. C. Ho, H. J. Rideout, E. Ribe, C. M. Troy, and W. T. Dauer, "The Parkinson Disease Protein Leucine-Rich Repeat Kinase 2 Transduces Death Signals Via Fas-Associated Protein With Death Domain and Caspase-8 in a Cellular Model of Neurodegeneration," *Journal of Neuroscience: The Official Journal of the Society for Neuroscience* 29, no. 4 (2009): 1011–1016.

4. C. K. Deniston, J. Salogiannis, S. Mathea, et al., "Structure of LRRK2 in Parkinson's Disease and Model for Microtubule Interaction," *Nature* 588, no. 7837 (2020): 344–349.

5. A. Myasnikov, H. Zhu, P. Hixson, et al., "Structural Analysis of the Full-Length Human LRRK2," *Cell* 184, no. 13 (2021): 3519–3527 e10.

6. C. Iaccarino, C. Crosio, C. Vitale, G. Sanna, M. T. Carri, and P. Barone, "Apoptotic Mechanisms in Mutant LRRK2-Mediated Cell Death," *Human Molecular Genetics* 16, no. 11 (2007): 1319–1326.

7. R. Di Maio, E. K. Hoffman, E. M. Rocha, et al., "LRRK2 Activation in Idiopathic Parkinson's Disease," *Science Translational Medicine* 10, no. 451 (2018): eaar5429.

8. E. G. Vides, A. Adhikari, C. Y. Chiang, et al., "A Feed-Forward Pathway Drives LRRK2 Kinase Membrane Recruitment and Activation," *eLife* 11 (2022): e79771.

9. A. Oun, A. M. Sabogal-Guaqueta, S. Galuh, A. Alexander, A. Kortholt, and A. M. Dolga, "The Multifaceted Role of LRRK2 in Parkinson's Disease: From Human iPSC to Organoids," *Neurobiology of Disease* 173 (2022): 105837.

10. K. Melachroinou, E. Leandrou, P. E. Valkimadi, et al., "Activation of FADD-Dependent Neuronal Death Pathways as a Predictor of Pathogenicity for LRRK2 Mutations," *PLoS one* 11, no. 11 (2016): e0166053.

11. C. Morrison, "Constrained peptides' Time to Shine?" *Nature Reviews. Drug Discovery* 17, no. 8 (2018): 531–533.

12. R. L. Wallings and M. G. Tansey, "LRRK2 Regulation of Immune-Pathways and Inflammatory Disease," *Biochemical Society Transactions* 47, no. 6 (2019): 1581–1595.

13. L. G. Helton, A. Soliman, F. von Zweydorf, et al., "Allosteric Inhibition of Parkinson's-Linked LRRK2 by Constrained Peptides," *ACS Chemical Biology* 16, no. 11 (2021): 2326–2338.

14. D. Jennings, S. Huntwork-Rodriguez, A. G. Henry, et al., "Preclinical and Clinical Evaluation of the LRRK2 Inhibitor DNL201 for Parkinson's Disease," *Science Translational Medicine* 14, no. 648 (2022): eabj2658.

15. M. A. S. Baptista, K. Merchant, T. Barrett, et al., "LRRK2 Inhibitors Induce Reversible Changes in Nonhuman Primate Lungs Without Measurable Pulmonary Deficits," *Science Translational Medicine* 12, no. 540 (2020): eaav0820.

16. L. R. Kett, D. Boassa, C. C. Ho, et al., "LRRK2 Parkinson Disease Mutations Enhance Its Microtubule Association," *Human Molecular Genetics* 21, no. 4 (2012): 890–899.

17. E. Leandrou, E. Markidi, A. Memou, K. Melachroinou, E. Greggio, and H. J. Rideout, "Kinase Activity of Mutant LRRK2 Manifests Differently in Hetero-Dimeric vs. Homo-Dimeric Complexes," *The Biochemical Journal* 476, no. 3 (2019): 559–579.

Supporting Information

Additional supporting information can be found online in the Supporting Information section.